JOURNAL OF ORAL MICROBIOLOGY
2024, VOL. 16, 2322241
https://doi.org/10.1080/20002297.2024.2322241

Taylor & Francis
Taylor & Francis Group

RESEARCH ARTICLE

OPEN ACCESS Check for updates

Genetic characterization of glyoxalase pathway in oral streptococci and its contribution to interbacterial competition

Lin Zeng, Payam Noeparvar, Robert A. Burne and Benjamin S. Glezer

Department of Oral Biology, University of Florida College of Dentistry, Gainesville, FL, USA

ABSTRACT

Objectives: To analyze contributions to microbial ecology of Reactive Electrophile Species (RES), including methylglyoxal, generated during glycolysis.

Methods: Genetic analyses were performed on the glyoxalase pathway in Streptococcus mutans (SM) and Streptococcus sanguinis (SS), followed by phenotypic assays and transcription analysis.

Results: Deleting glyoxalase I (lguL) reduced RES tolerance to a far greater extent in SM than in SS, decreasing the competitiveness of SM against SS. Although SM displays a greater RES tolerance than SS, lguL-null mutants of either species showed similar tolerance; a finding consistent with the ability of methylglyoxal to induce the expression of lguL in SM, but not in SS. A novel paralogue of lguL (named gloA2) was identified in most streptococci. SM mutant ΔgloA2SM showed little change in methylglyoxal tolerance yet a significant growth defect and increased autolysis on fructose, a phenotype reversed by the addition of glutathione, or by the deletion of a fructose: phosphotransferase system (PTS) that generates fructose-1-phosphate (F-1-P).

Conclusions: Fructose contributes to RES generation in a PTS-specific manner, and GloA2 may be required to degrade certain RES derived from F-1-P. This study reveals the critical roles of RES in fitness and interbacterial competition and the effects of PTS in modulating RES metabolism.

ARTICLE HISTORY
Received 6 January 2024
Revised 8 February 2024
Accepted 16 February 2024

KEYWORDS
Reactive electrophile species; methylglyoxal; dental caries; *Streptococcus mutans*; phosphotransferase system (PTS); competition

Introduction

The initial pathway for catabolism of carbohydrates for energy production is the Embden-Meyerhof-Parnas pathway, often referred to as glycolysis. Incoming carbohydrates are phosphorylated and, by the activities of a series of enzymes conserved in both bacteria and mammalian cells, converted into pyruvate and a cohort of metabolic intermediates that are critical to bacterial growth and metabolism [1]. Either catalyzed by specific enzymes or produced as the byproducts of various non-enzymatic reactions, reactive electrophile species (RES), including two prominent dicarbonyl compounds, methylglyoxal (MG) and glyoxal (GO), are created during metabolism of carbohydrates, proteins or lipids [2]. These RES metabolites are often produced in significant quantities in cells actively engaged in carbohydrate metabolism, or in diabetic patients experiencing poor metabolic/glycemic control [3]. Due to their biochemical properties, RES are membrane-permeable and highly reactive towards most cellular macromolecules, including proteins, nucleic acids and lipids [4,5]. These reactions can significantly alter the nature and functions of affected biological molecules, and often result in the creation of other reactive intermediates and advanced glycation end-products (AGEs); both RES and AGEs are implicated in the pathophysiology of chronic conditions such as aging, diabetes and cancer development [6]. For example, MG and GO contribute to the progression of type 2 diabetes (T2DM) and development of its many complications, such as kidney diseases (diabetic nephropathy), vision (retinopathy) and neurological damages [3]. Because of their reactivity, the majority of RES are present in bound forms to biological molecules, so their abundance is frequently underestimated [7]. Significantly, high levels of MG have been reported after treatment of the periodontal pathogen *Tannerella forsythia* with glucose, or during infection of macrophages by certain mycobacteria [8,9].

While most bacteria have the necessary apparatus to detoxify and degrade MG and GO, some (e.g. *Escherichia coli, Bacillus subtilis*) actively engage in biosynthesis of MG as a mechanism, termed methylglyoxal bypass, to control glycolytic rates, especially under high-carbohydrate or low-phosphate conditions [4,10,11]. In this process, a metabolic intermediate of glycolysis, dihydroxyacetone phosphate (DHAP) is dephosphorylated and converted into MG, which upon a spontaneous reaction with the reduced form of glutathione (GSH), forms a hemithioacetal that is then converted into S-lactoylglutathione (SLG) by the

CONTACT Lin Zeng lzeng@dental.ufl.edu Department of Oral Biology, University of Florida College of Dentistry, 1395 Center Drive, D5-27, Gainesville, FL 32610, USA

Supplemental data for this article can be accessed online at https://doi.org/10.1080/20002297.2024.2322241

activity of glyoxalase I. SLG is subsequently converted into D-lactate and GSH via the activity of glyoxalase II. D-lactate can then be oxidized by a unique D-lactate dehydrogenase to pyruvate to end the MG bypass. SLG can also serve as an important allosteric effector that activates a potassium: proton antiporter KefGB of *E. coli*, which in turn acidifies the cytoplasm and enhances RES tolerance [12]. However, most Gram-positive species lack the enzyme required for biosynthesis of MG, methylglyoxal synthase (MgsA) [13,14]. Instead, glyoxalases I and II in these bacteria work in concert to degrade MG originating exogenously or created by endogenous metabolic activities, during which the activity of glyoxalase I is often the rate-limiting step [12,15,16]. Furthermore, because of the need for GSH during the metabolism of MG, exposure to MG can disrupt the redox homeostasis of GSH and glutathione disulfide (GSSG) [17].

Recent advances have highlighted the complex interplay between human microbiomes and systemic health. With T2DM affecting close to 10% of the world's adult population [18], there is an urgent need for better understanding of the influence of the pathophysiological state of T2DM on the genomics, biochemistry and ecology of the human microbiome. For example, studies of periodontal diseases in the context of diabetes have established a two-way relationship between T2DM and microbiome dysbiosis that is often the driving force behind deteriorating periodontal health [19]. For dental caries, there has been an increasing body of evidence associating poor glycemic control with increased risk for dental caries [20–25]. As such, more in-depth research is needed to address the impact of increased excretion of RES on microbial homeostasis in the context of dental caries. As the most abundant members of the supragingival microbiota and potent producers of organic acids, streptococci contribute directly to dental health and diseases by shaping the taxonomic and biochemical landscape of the biofilm [26–28]. In this report, we performed genetic analysis on several genes whose products are essential to RES tolerance of a model caries pathobiont, *Streptococcus mutans*, and a commensal competitor *Streptococcus sanguinis*. Our study revealed the ability of RES to influence streptococcal competition due to significant difference in resistance levels and response in gene regulation by individual species, as well as the interconnected nature of sugar: phosphotransferase system (PTS) and RES metabolism.

Results and discussion

Identification of putative MG metabolic genes in streptococci

Apart from biochemical studies in the model microorganisms *E. coli* and *B. subtilis*, relatively little is known regarding the contribution and regulation of MG metabolism in microbial pathogenesis [3]. To begin to better understand MG metabolism in the oral microbiome, we conducted a search for putative MG synthetic and metabolic genes in several relevant streptococci, including *S. mutans* (SM), *S. sanguinis* (SS), *Streptococcus gordonii* (SG), *Streptococcus mitis* and *Streptococcus pneumoniae*, etc. As depicted in Figure 1, in addition to genes predicted to encode for glyoxalase I (*lguL/gloA1*) and glyoxalase II (*gloB*), another glyoxalase I paralogue (tentatively named *gloA2*) was identified in most Gram-positive species analyzed other than *S. mitis* and *S. pneumoniae*. *gloA2* orthologues were also identified in isolates of *E. coli* as an uncharacterized gene. Aside from *Enterococcus faecalis*, most lactic acid bacteria do not appear to harbor a gene for MG synthase (*mgsA*).

In comparison, $GloA2_{SM}$ and $LguL_{SM}$ are 29% identical in sequence. The crystal structure of $GloA2_{SM}$ has been solved (Protein Data Bank, RCSB PDB 3L7T). It is a Zn^{2+}-binding protein predicted to be active as a homodimer. $GloA2_{SM}$ and the predicted structure of $LguL_{SM}$ show high degrees of structural similarity (Figures 2 and S1). Although further functional study is required to fully characterize $GloA2_{SM}$ and its homologs, these results support the notion that both proteins may function in RES metabolism. In *S. mutans* and several other streptococci, *lguL* (SMU.1603) forms an apparent operon structure with another ORF encoding a putative NAD(P)H-flavin oxidoreductase (SMU.1602) (Figure 1), a conclusion supported by our RT-qPCR (below) and multiple publications of transcriptomic and proteomic analyses that showed co-regulation of these two genes under various conditions [29,30]. Downstream and in opposite orientation to that of SMU.1602–1603 is a putative transcription regulator, SMU.1604c that shares homology with the PadR family repressors [31]. Adjacent to SMU.1604c and in opposing orientation is SMU.1605, a putative transmembrane protein sharing homology with a drug efflux pump of *Bacillus*. Notably different from SMU.1602–1604c, no transcription regulator gene was identified in similar locations in other streptococci. Incidentally, SMU.1604c was also crystallized and determined to be an Mg^{2+}-binding protein (RCSB PDB 3L9F).

Genetic analyses in S. mutans and S. sanguinis of genes required for MG metabolism

To assess the genetic structure and function of each gene/ORF predicted to degrade MG, individual deletions were engineered in *S. mutans* strain UA159 by knocking out $gloA2_{SM}$, $lguL_{SM}$ and $gloB_{SM}$, followed by phenotypic characterization associated with RES tolerance. At the same time, deletions of equivalent

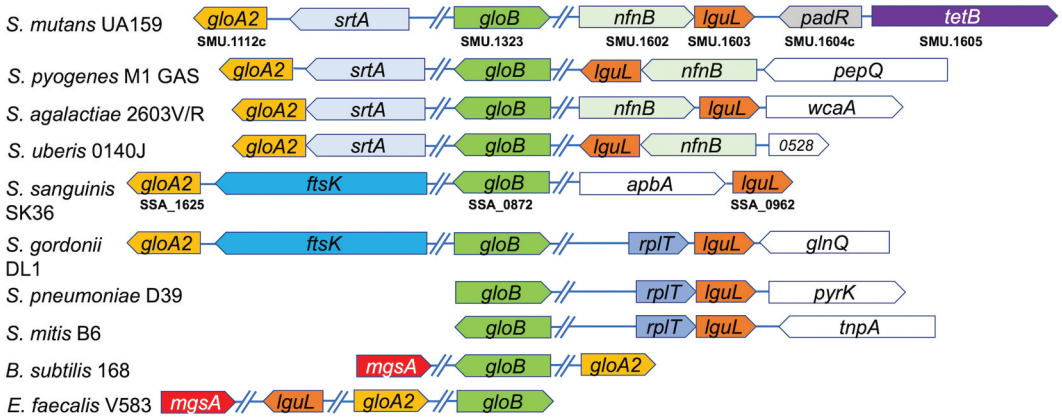

Figure 1. Genetic organization of genes/ORFs likely involved in MG metabolism in relevant Gram-positive bacteria. Bacteria depend on the glyoxalase pathway for metabolism of MG and GO, a two-step reaction that is catalyzed by gene products of *lguL*/*gloA1* (SMU.1603 and SSA_0962) and *gloB* (SMU.1323 and SSA_0872). Based on sequence and structure similarity (Figure 2), a paralogue of *lguL, gloA2* (SMU.1112c and SSA_1625), with no known function has been identified in most species analyzed.

genes, $gloA2_{SS}$, $lguL_{SS}$ and $gloB_{SS}$, were constructed similarly in the background of *S. sanguinis* SK36. These deletion mutants were analyzed in planktonic growth assays utilizing a synthetic medium (FMC) supplemented with MG or GO, and minimum inhibitory concentrations (MICs) for MG or GO were determined by a micro-dilution assay in FMC.

Relative to the wild-type UA159 (SM), deletion of $lguL_{SM}$ resulted in a reduction in tolerance to MG (Table 1) from 5.5 mM to 1.5 mM (~75%), and an extended lag phase in FMC-glucose supplemented with 1 mM of MG (Figure 3). These results confirmed previous studies [13,14] that suggested that LguL is the major GloA enzyme responsible for degrading MG in streptococci. However, different from a previous report on *lguL* in *S. mutans* [14], strain $\Delta lguL_{SM}$ did not show any significant change in its ability to grow in FMC-glucose adjusted to pH 5.5 or 6.0, or in THYE at pH 7.5 or 5.0, nor did any other mutants analyzed here (Figure S2). Also consistent with previous findings in other bacterial systems [15], loss of SMU.1323, encoding a putative GloB enzyme, resulted in no reduction in MG tolerance.

Deletion of $gloA2_{SM}$ slightly reduced the MIC for MG (from 5.5 mM to 4.5 mM). Deletion of $gloA2_{SM}$ or $gloB_{SM}$ in the background of strain $\Delta lguL_{SM}$ did not further increase its susceptibility to MG. Surprisingly, strain $\Delta gloA2_{SM}$ grew significantly better in planktonic growth curve assays than the wild type did on FMC-glucose containing 1 mM MG, with a shorter lag phase, faster growth rate and higher final optical density (Figure 3). $\Delta gloA2_{SM}$ also grew slightly better than the wild type on glucose without the addition of MG. It appears that the functionality of $GloA2_{SM}$ in MG resistance is significantly influenced by the condition in which MIC assays were performed using static cultures maintained in ambient atmosphere supplemented with 5% CO_2, whereas the cultures

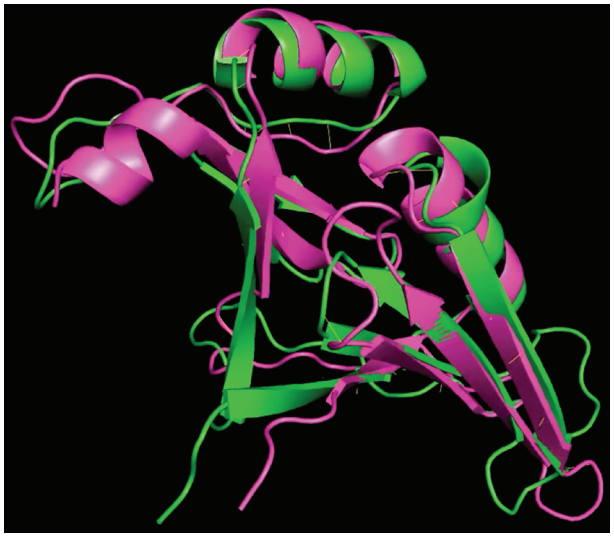

Figure 2. Structure overlay between proteins $GloA2_{SM}$ (green) and $LguL_{SM}$ (purple). The structure of $LguL_{SM}$ was rendered using Alphafold 2.

for growth curve assays were covered by mineral oil and no additional CO_2 in the atmosphere, but briefly shaken once every hour. To confirm the contribution of $gloA2_{SM}$ to MG tolerance in SM, a high-copy-number plasmid pIB184 [34] was used to express $gloA2_{SM}$ under a constitutive promoter. However, no increase in MG tolerance was noted when this plasmid (pIB-1112c) was introduced to the backgrounds of UA159, $\Delta gloA2_{SM}$ or $\Delta lguL_{Sm}$ (data not shown). Therefore, it appears unlikely that MG is a specific substrate for $GloA2_{SM}$.

Interestingly, two important commensal streptococci, *S. sanguinis* and *S. gordonii*, were significantly less tolerant to treatment by MG (Table 1, Figure S3). Similar to UA159 (SM), deletion of SSA_0962/$lguL_{SS}$ in the background of SK36 (SS) resulted in lower MIC values for MG (Table 1) when growing in FMC-glucose. Notably different

Table 1. MIC (minimum inhibitory concentrations) of MG and GO measured in wild-type oral streptococcal strains and mutant derivatives. Each result is presented as a range to denote both the average MIC (first number) and the next increment of concentration. Three biological replicates were used to calculate the MIC range for each strain.

Standard Lab Strains	MG MIC range (mM)	GO MIC range (mM)	Other WT *S. mutans* strains	MG MIC range (mM)	Oral Commensal isolates	MG MIC range (mM)
UA159 (SM)	5.5–6	1.8–2.1	SM UA101	3.5–4	BCC03[a]	1.9–2.2
Δ$manL_{SM}$	7–7.5	2.7–3.0	SM GS-5	4.5–5	BCC05[b]	<1
Δ$gloA2_{SM}$::*Km*	4.5–5	1.8–2.1	SM 10449	3.5–4	BCC06[c]	<1
Δ$gloA2_{SM}$::*Em*	4.5–5	1.8–2.1	SM ST1	5.5–6	BCC07[c]	<1
Δ$gloA2_{SM}$Com	4.5–5	1.5–1.8	SM SM6	4.5–5	BCC09[d]	2.8–3.1
Δ$gloB_{SM}$	6–6.5	1.8–2.1	SM OMZ175	5–5.5	BCC10[b]	1.6–1.9
Δ$lguL_{SM}$	1.5–2	0.6–0.8	SM U2A	4–4.5	BCC11[e]	1.9–2.2
Δ$lguL_{SM}$Com	5.5–6	1.8–2.1			BCC14[a]	1.6–1.9
Δ$gloA2_{SM}$/$lguL_{SM}$	1.5–2	ND			BCC15[f]	1–1.3
Δ$gloB_{SM}$/$lguL_{SM}$	1.5–2	ND			BCC19[e]	2.2–2.5
Δ*gshAB*::*Km*	2.5–3	1.4–1.6			BCC21[g]	2.2–2.5
Δ*gshAB*::*Em*	3–3.5	ND			BCC23[a]	1.9–2.2
Δ*gshAB*Com	5–5.5	ND			BCC26[b]	1.9–2.2
SK36 (SS)	2.25–2.5	0.8–0.9			BCC27[d]	3.4–3.7
Δ$manL_{SS}$	1.75–2	ND				
Δ$lguL_{SS}$	1.75–2	0.6–0.7				
Δ$gloB_{SS}$	2.25–2.5	0.8–0.9				
Δ$gloA2_{SS}$	2.25–2.5	0.8–0.9				
Δ$gloA2_{SS}$/$lguL_{SS}$	1.75–2	0.6–0.7				
SG DL1	2.25–2.5	0.8–1.0				
Δ$manL_{SG}$	1.75–2	ND				

ND, not determined. [a]*S. sanguinis*; [b]*S. dentisani*; [c]*S. mitis*; [d]*S. gordonii*; [e]*S. oralis*; [f]*S. parasanguinis*; [g]*Streptococcus* sp. A12 [32,33].

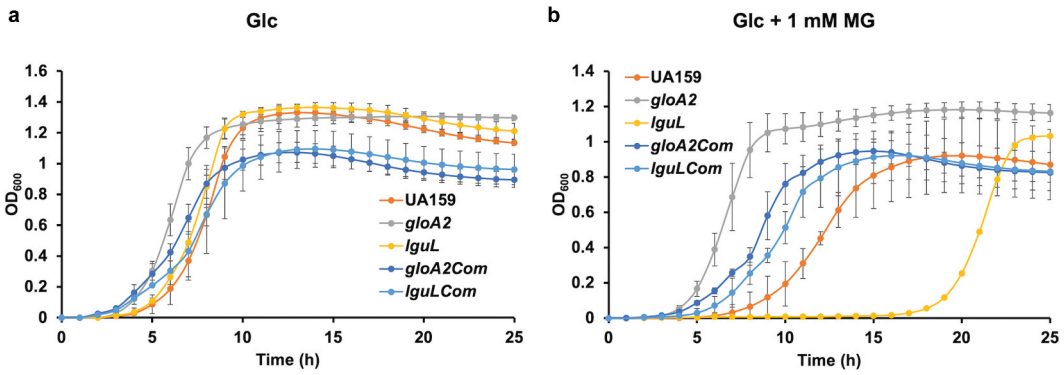

Figure 3. Growth curves of SM strain UA159 and its isogenic mutants deficient in $gloA2_{SM}$ or $lguL_{SM}$. Bacterial cultures prepared with BHI were diluted into a synthetic FMC medium constituted with 20 mM of glucose and 0 (a) or 1 mM (b) of MG. Each strain was represented by at least three individual cultures, with error bars denoting the standard deviations. All cultures were covered with sterile mineral oil and incubated at 37°C for monitoring of optical density at 600 nm (OD_{600}).

from SM was the fact that deletion of $lguL_{SS}$ resulted in less than a 1-mM reduction in MIC for MG, as opposed to a 4-mM drop caused by deletion of $lguL_{SM}$, although strains Δ$lguL_{SS}$ and Δ$lguL_{SM}$ now have similar tolerance against MG. Deletion of $gloA2_{SS}$, the orthologue of $gloA2_{SM}$, failed to show any change in MG tolerance. We further expanded the MIC assay to include seven additional wild-type SM isolates and 14 clinical isolates of various species of commensal streptococci. The results (Table 1) showed that, compared to most commensal streptococcal species tested, each *S. mutans* strain was significantly more tolerant to MG. Last, likely more reactive than MG by having two aldehyde groups, glyoxal (GO) exerted greater growth inhibition than MG when used at the same levels (Table 1). Again UA159 (SM) was notably more tolerant to GO than SK36 (SS) or DL1 (SG), and genetic deletions that altered MG tolerance in both SM and SS similarly impacted relative tolerance to GO, except for *gloA2*, a finding consistent with their chemical similarity and likely shared pathways that bacteria use for detoxification [2]. Thus, there appears to be a significant difference in the contributions of *lguL* gene products to MG tolerance among oral streptococci.

$GloA2_{SM}$ and PTS are involved in RES metabolism in a metabolite-specific manner

To better understand the phenotypes of strain Δ$gloA2_{SM}$, further analyses were carried out by growing it on different carbohydrates. When observed under the microscope, Δ$gloA2_{SM}$ cells presented significantly longer chain length than the

wild type, clumped into clusters/aggregates, and tended to fall out of the culture media (Figure 4(a)). This phenotype was apparent in liquid BHI medium and FMC-fructose, but not in FMC containing other tested carbohydrates (Figure S4). As cell chaining and clustering are often associated with stress and autolysis, we then tested these mutant derivatives in growth and autolysis assays using fructose as the supporting carbohydrate. As shown in Figure 5(a,b), Δ*gloA2*$_{SM}$ had a slower growth rate and a lower final yield than the wild type, as well as lower CFU counts from the same cultures. When these strains were subjected to an autolysis assay by incubating at 44°C, Δ*gloA2*$_{SM}$ cultures prepared with fructose showed a significantly faster decline in optical density when compared to the wild type or the complemented strain (Figure 5(c)). When measurements of extracellular DNA (eDNA) were obtained by reacting with a fluorescent DNA dye [35], the culture supernates of Δ*gloA2*$_{SM}$ showed significantly higher levels of eDNA than the wild type after 24-h in fructose-based medium (Figure 5(d)), consistent with the notion of increased cell lysis. Also, development of biofilms' formation by UA159 (SM) was negatively affected by the deletion of *gloA2*$_{SM}$ in a 48-h biofilm assay using BM medium containing 2 mM sucrose in addition to 18 mM of glucose or fructose (Figure S5). To contrast the phenotype of Δ*gloA2*$_{SM}$ with wild-type cells under RES stress, we treated exponentially growing UA159 (SM) cells with 1 mM MG. After 70 min of incubation, cells treated with MG showed a slight but consistent increase in chain length under the microscope (Figure 4(b)).

Our previous research on fructose metabolism by *S. mutans* [35,36] showed the significance of fructose-1-phosphate (F-1-P) as a potential stress signal that led to enhanced autolysis and release of DNA, although the mechanism remains to be clarified. To test the theory that the growth phenotype of strain Δ*gloA2*$_{SM}$ is influenced by F-1-P accumulation, we deleted the PTS EII permease, FruI, that is responsible for generating most of F-1-P in *S. mutans* [35] in the *gloA2*$_{SM}$-null background. A mutant lacking another fructose-PTS transporter, LevDEFG [37] which yields F-6-P, in the *gloA2*$_{SM}$-null background was also included for comparison. Loss of *fruI*, but not *levD*, reversed the growth phenotype of Δ*gloA2*$_{SM}$ in fructose-based medium (Figure S6), including the growth rate and yield (Figure 5(a)), and extent of chaining (Figure 6). In fact, the chain length of Δ*gloA2*$_{SM}$/*fruI* was considerably shorter than that of the wild type, a result echoed what was reported previously in Δ*fruI*$_{SM}$ background [35]. Regarding the phenotype of Δ*gloA2*$_{SM}$ when growing on BMGS and BHI, it has been demonstrated that sucrose catabolism by *S. mutans* often leads to release of free fructose; BHI medium contains a small amount of fructose contaminant [38,39].

We next tested the possibility that F-1-P mediated stress phenotype involves RES generation, which requires the activity of GloA2$_{SM}$ for detoxification. It is understood that fructose, when metabolized as F-1-P, can bypass the allosteric regulation exerted onto the phosphofructokinase (PFK-1) during glycolysis that uses F-6-P as a substrate, resulting in faster generation of RES [40]. Further, research has suggested that oxidative degradation of fructose under the influence of Fenton reaction, i.e. hydrogen peroxide (H_2O_2) in the presence of Fe^{2+}, strongly potentiates the creation of RES compound GO and fructose-mediated cytotoxicity in mammalian cells [41,42]. Since reduced glutathione (GSH) is the substrate required for detoxification of MG and GO, we added varying amounts of GSH to the cultures of Δ*gloA2*$_{SM}$ in FMC-fructose. When observed under the microscope, GSH reversed the clumping phenotype of Δ*gloA2*$_{SM}$ in a dose-dependent manner (Figure 7); addition of GSH also partially rescued its growth phenotype on fructose (Figure 5(a)). Last, we tested a deletion mutant of UA159 (SM) deficient in glutathione synthetase (*gshAB*) [43] in its RES tolerance. The result showed an MIC for MG at 2.5–3 mM, a level slightly higher than Δ*lguL*$_{SM}$, but significantly lower than the wild-type parent (Table 1). Therefore, it appears that the fitness phenotype of strain Δ*gloA2*$_{SM}$ involves F-1-P and the depletion of cellular GSH pools. However, since strain Δ*lguL*$_{SM}$ does not display a similar phenotype when grown with fructose, nor does strain Δ*gloA2*$_{SM}$ display GO sensitivity, the mechanism by which GloA2$_{SM}$ confers protection against the metabolites of F-1-P likely differs from that of glyoxalases I and II as we understand. Alternatively, degradation of F-1-P by certain aldolase could result in production of DHAP and glyceraldehyde, the latter of which is another-although considerably less reactive than MG or GO-electrophile species that can react with GSH [44]. We plan to explore the possibility of glyceraldehyde as a substrate of GloA2$_{SM}$ in the near future.

To study the role of *gloA2* orthologue in commensal streptococci, deletion mutant of *gloA2*$_{SS}$ in SS was compared to the wild-type SK36 (SS) for growth on different carbohydrates. Relative to UA159 (SM), SK36 (SS) released greater amounts of eDNA when growing on fructose and had lower persistence when the CFUs of the cultures were compared (Figure 5(b,c)). Like its counterpart in SM background, cells of strain Δ*gloA2*$_{SS}$ fell out of solution in BHI cultures, had longer chain length and clumped under the microscope (Figure S7). Interestingly, while strain Δ*gloA2*$_{SM}$ grew very poorly on fructose (but not on mannose), strain Δ*gloA2*$_{SS}$

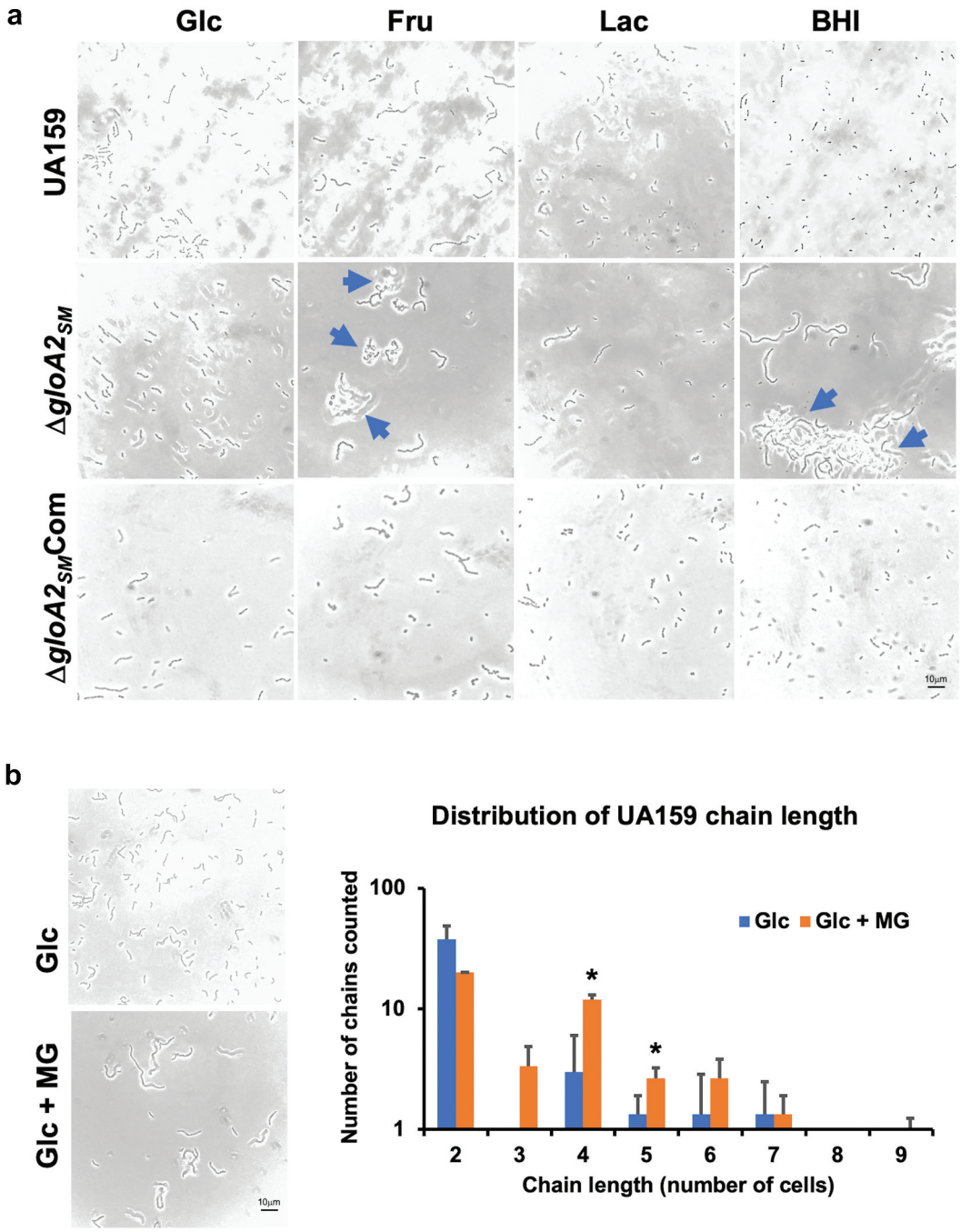

Figure 4. Phase-contrast microscopy. (a) SM Strains UA159, Δ*gloA2*$_{SM}$ and Δ*gloA2*$_{SM}$Com were each cultured in BHI, or FMC with glucose (Glc), fructose (Fru), or lactose (Lac) overnight. Arrows highlight the clumping phenotype. (b) Exponential-phase cultures of UA159 (n = 3, OD_{600} = 0.4) prepared in FMC with Glc were treated with 1 mM MG for 70 min. Distribution of bacterial chain length was assessed by counting 50 random chains in each sample under the microscope (Student's *t*-test; *$P < 0.05$).

showed only a minor deficiency growing on fructose, yet a more significant deficiency on mannose (Figure S6). Further, deletion of a *fruI* orthologue in Δ*gloA2*$_{SS}$ background failed to reverse the phenotype on mannose, although mannose (in the form of mannose-6-P) is known to be first converted to F-6-P once internalized by *S. mutans* [45]. Interestingly, SK36 (SS) released the most eDNA growing on mannose in comparison to glucose or fructose (Figure S7). Further research is needed to elucidate the different roles played by these two *gloA2* orthologues in fructose- and mannose-mediated stress phenotypes in these two important oral streptococci.

Another PTS of critical importance to the pathophysiology of *S. mutans* is the glucose/mannose-PTS (EII^{Man}, *manLMNO*), a major transporter for glucose and multiple other carbohydrates, but not fructose [46]. A mutant lacking the *manL* gene (Δ*manL*$_{SM}$) was tested for RES tolerance. Different from mutants of the glyoxalase pathway, Δ*manL*$_{SM}$ showed enhanced resistance to both MG and GO when included in the MIC assay (Table 1).

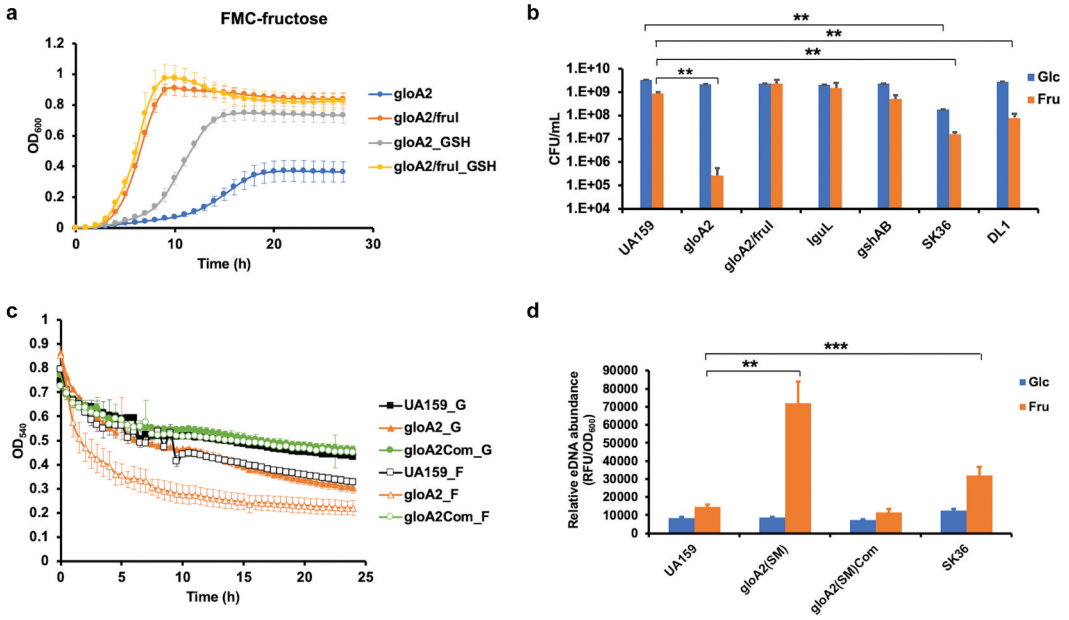

Figure 5. Phenotypic characterization of mutants deficient in methylglyoxal and related metabolic genes. (a) Growth curves of strains Δ*gloA2*$_{SM}$ and Δ*gloA2*$_{SM}$/*fruI* in FMC supported with 20 mM fructose, with or without 1 mM GSH. Error bars represent standard deviations. (b) CFU counts of 24-h bacterial cultures in FMC supported with 20 mM glucose or fructose. (c) Autolysis assay. The strains were cultured in TV media containing 20 mM of glucose (_G) or fructose (_F) till OD_{600} = 0.7, washed twice with PBS, resuspended in autolysis buffer [56], and monitored in a Bioscreen C system that was maintained at 44°C and set to shake for 15s before measurement every 30 min. (d) Relative eDNA abundance in 24-h cultures in FMC supported with glucose or fructose, normalized against the final OD_{600}. Each sample was represented by at least three independent cultures. Asterisks denote statistical significance assessed by Student's *t*-test (*P < 0.05; **P < 0.01; ***P < 0.001; ****P < 0.0001).

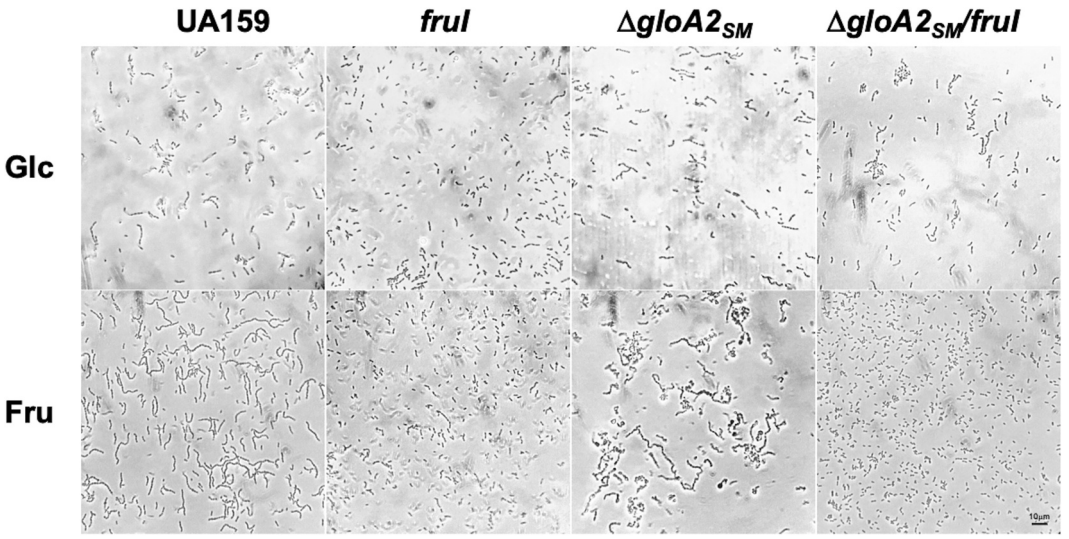

Figure 6. Loss of a F-1-P-generating PTS (Fru) reversed the phenotype of Δ*gloA2*$_{SM}$. Overnight cultures (n = 3) of strain Δ*gloA2*$_{SM}$ in FMC with 20 mM Glc or Fru were subjected to phase-contrast microscopy.

Additional analysis of the unique phenotype of strain Δ*manL*$_{SM}$ was carried out below.

Treatment with MG significantly alters bacterial gene expression

To understand the impact of MG at the molecular level, UA159 (SM) and SK36 (SS) were each grown in FMC-glucose to exponential phase and treated with sub-MIC levels of MG for 30 min before harvesting. RT-qPCR assays were carried out in these cells to measure the mRNA levels of genes of the glyoxalase pathway and those deemed critical to persistence. As shown in Table 2, treatment of UA159 (SM) with MG resulted in increased expression of the putative SMU.1602–1603/*lguL* operon (more than twofold), superoxide dismutase (*sod*, sevenfold) [47], glutathione synthetase (*gshAB*, twofold) and a fructose-inducible *rcrRPQ* operon (twofold) that is important for *S. mutans* aerobic stress

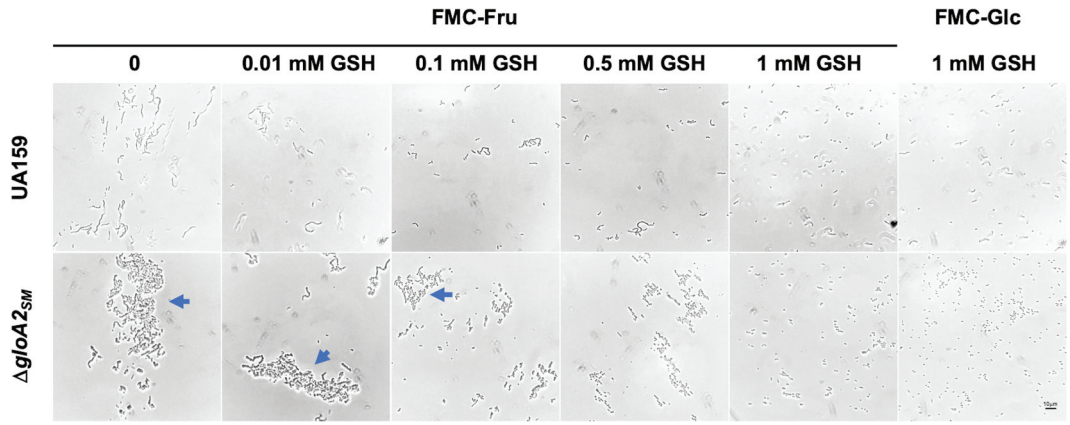

Figure 7. Addition of glutathione (GSH) reversed the phenotype of Δ*gloA2*$_{SM}$ on fructose. Strain Δ*gloA2*$_{SM}$ was cultivated overnight with GSH ranging from a concentration of 0–1 mM, before being observed under microscope. Arrows indicate the clumping phenotype.

tolerance and competence [48,49]. The transcript levels of *gloA2*$_{SM}$ remained unchanged, while that of *gloB*$_{SM}$ showed a slight reduction. Most genes required for central carbon metabolism and PTS, including pyruvate formate lyase (*pfl*), pyruvate dehydrogenase complex (*pdh*), acetate kinase (*ackA*), glycogen synthase operon (*glg*), glucose-PTS operon (*man*), PTS EI (*ptsI*) and HPr (*ptsH*) were substantially downregulated by the treatment. Considering the effect of fructose on *gloA2*$_{SM}$ mutants, we also analyzed RNA samples extracted from UA159 (SM) grown with fructose. The limited analysis so far showed elevated expression of the SMU.1602–1603/*lguL* operon in the presence of fructose at levels similar to treatment with MG (approximately twofold). Together, these findings suggested that MG-induced gene regulation in SM could overlap with that mediated by fructose treatment, especially via the F-1-P pathway. Considering the conservation of both *gloA2* and *fruI* in many streptococci and the role of GSH::GSSG balance in bacterial physiology, such a regulation could also be involved in stress response or interaction with host immunity.

In comparison, treatment of SK36 (SS) with MG resulted in reduced expression in bioenergetic genes *pfl* and *ldh* (lactate dehydrogenase), although *pdh*, *spxB* (pyruvate oxidase) and *nox* (NADH oxidase) each showed a slight increase in mRNA levels (Table 2). Significantly different from UA159 (SM), mRNA

Table 2. RT-qPCR results showing the relative abundance of mRNA levels of important genes. Each strain was grown to exponential phase (OD_{600} = 0.5) and treated with MG (at 5 mM for SM and 2 mM for SS) for 30 min. Each strain was represented by at least three individual cultures, and each cDNA was measured in technical duplicates. The results are each presented as average and standard deviation (in parentheses). The statistical significance of each MG-treated strain was assessed against the same strain grown without MG, and for Δ*manL*$_{SM}$ grown without MG, against UA159 without MG. Asterisks denote statistical significance according to Student's *t* test (*P < 0.05; **P < 0.01; ***P < 0.001; ****P < 0.0001).

	UA159 (SM)		Δ*manL*$_{SM}$			SK36 (SS)	
Genes	no MG	5 mM MG	no MG	5 mM MG	Genes	no MG	2 mM MG
gloA2$_{SM}$	1.00 (0.11)	1.11 (0.13)	0.90 (0.07)	0.89 (0.07)	*gloA2*$_{SS}$	1.00 (0.03)	0.70 (0.10)*
lguL$_{SM}$	1.01 (0.14)	2.73 (0.19)****	1.26 (0.16)	3.01 (0.40)**	*lguL*$_{SS}$	1.00 (0.05)	0.28 (0.02)***
SMU.1602	1.00 (0.03)	3.39 (0.36)**	1.21 (0.12)	3.45 (1.19)			
gloB$_{SM}$	1.00 (0.06)	0.81 (0.05)*	0.86 (0.05)*	0.54 (0.03)***	*gloB*$_{SS}$	1.00 (0.02)	0.52 (0.005)***
gshAB	1.00 (0.08)	1.93 (0.18)**	1.02 (0.04)	1.69 (0.47)			
sod	1.00 (0.02)	7.36 (0.75)**	1.29 (0.04)**	7.90 (2.50)*			
pfl$_{SM}$	1.00 (0.06)	0.20 (0.01)***	1.69 (0.11)***	0.46 (0.01)***	*pfl*$_{SS}$	1.00 (0.06)	0.12 (0.02)**
pdhD$_{SM}$	1.10 (0.63)	0.37 (0.06)	5.64 (0.63)***	3.10 (0.10)**	*pdhA*$_{SS}$	1.023 (0.26)	1.88 (0.71)
manN	1.01 (0.14)	0.37 (0.05)**	1.367 (0.12)*	0.34 (0.01)*8	*manL*	1.001 (0.08)	0.73 (0.63)
ackA$_{SM}$	1.01 (0.14)	0.55 (0.07)*	1.22 (0.08)	0.96 (0.27)	*ackA*$_{SS}$	1.00 (0.06)	1.43 (0.43)
gtfB	1.00 (0.07)	0.66 (0.05)**	0.79 (0.11)	0.33 (0.07)**	*spxB*	1.00 (0.05)	1.87 (0.85)
glnQ	1.00 (0.11)	0.38 (0.09)**	1.11 (0.18)	0.11 (0.01)**	*pflA*	1.00 (0.08)	0.85 (0.10)
ptsH	1.00 (0.08)	0.15 (0.01)**	0.89 (0.09)	0.1 (0.02)**	*nox*	1.00 (0.06)	1.90 (0.56)
dnaK	1.01 (0.16)	0.31 (0.05)*	1.48 (0.27)	0.16 (0.03)*	*ldh*	1.02 (0.29)	0.41 (0.08)*
glgD	1.01 (0.16)	0.39 (0.07)*	1.73 (0.17)**	0.76 (0.08)**	*pykF*	1.05 (0.43)	0.83 (0.18)
rcrR	1.00 (0.03)	1.88 (0.55)					
rcrP	1.00 (0.02)	2.22 (0.31)*					
relA	1.00 (0.04)	1.25 (0.17)					
relP	1.00 (0.02)	0.90 (0.56)					
relQ	1.00 (0.04)	0.43 (0.02)***					
sloA	1.00 (0.06)	0.25 (0.02)***					
citB	1.01 (0.18)	0.27 (0.04)*					

levels of the orthologue of *lguL* (SSA_0962) in SK36 (SS) were reduced twofold by the treatment with MG. Together, these results suggested that MG treatment at sub-MIC levels inhibits the central metabolism that is required for energy production and anabolism in both bacteria, yet triggers different responses in terms of the glyoxalase pathway: *lguL* orthologue is induced in SM but suppressed in SS background. This could at least partly explain the greater tolerance to RES shown by the pathobiont than the commensal SS. As depicted in Figure 1, the genetic structure surrounding $lguL_{SM}$ appears significantly different from most oral streptococci.

To understand how the glucose-PTS mutant of UA159, $\Delta manL_{SM}$ presents enhanced RES resistance, the same treatment and RT-qPCR analysis were performed on SM mutant $\Delta manL_{SM}$. When treated with MG, $\Delta manL_{SM}$ showed (Table 2) wild-type levels of expression by $gloA2_{SM}$, $lguL_{SM}$, SMU.1602, *gshAB, sod* and several other pathways. However, unlike the wild type, increased expression of several metabolic pathways/genes, *glgD, pfl*, but chiefly the *pdh* operon [50], was observed, revealing superior energy management under RES stress and providing a plausible explanation for enhanced RES tolerance by the *manL* mutant. Previous research using *S. mutans* suggested that an intact PDH complex is essential to bacterial survival under stress such as extended starvation [51] and acidic conditions [52]. Notably different from the *manL* mutant of UA159 (SM), similarly constructed glucose-PTS (*manL*) mutants in the backgrounds of SK36 (SS) and DL1 (SG) each showed a slight reduction in MG tolerance (Table 1 and Figure S3).

MG metabolism influences interspecies competition

An important objective of this study was to assess the effect of RES on microbial interactions between *S. mutans* and commensals. A growth competition between UA159 (SM) and SK36 (SS), each labeled with a different antibiotic marker, was carried out in a planktonic culture prepared using FMC supplemented with glucose or fructose, with or without addition of MG. As indicated in Figure 8, when co-cultured without MG, both species appeared comparable in competitiveness, either in glucose- or fructose-based medium. However, when 1 mM MG was added to the media, UA159 (SM) showed 20 ~ 170-fold increases in competition indices depending on the carbohydrate, a result consistent with our earlier finding that UA159 (SM) is significantly more resistant to MG than SK36 (SS).

We then tested the role of $GloA2_{SM}$ and $LguL_{SM}$ in this competition by replacing the wild-type UA159 (SM) with their respective mutants. As shown in Figure 8, loss of $gloA2_{SM}$ resulted in little change to the relative competitiveness between these two species in FMC-glucose, regardless of the presence of MG. However, in FMC-fructose, strain $\Delta gloA2_{SM}$ was markedly less competitive relative to the wild type, showing a ~ 3000-fold reduction in competition indices without MG, but an even greater reduction (~11,000-fold) when treated with 1 mM MG. This outcome echoed our earlier conclusion that $GloA2_{SM}$ is primarily responsible for fitness when fructose is the primary growth carbohydrate but may also deal with RES stress. Conversely, when strain $\Delta lguL_{SM}$ was used to substitute UA159 (SM), little difference was

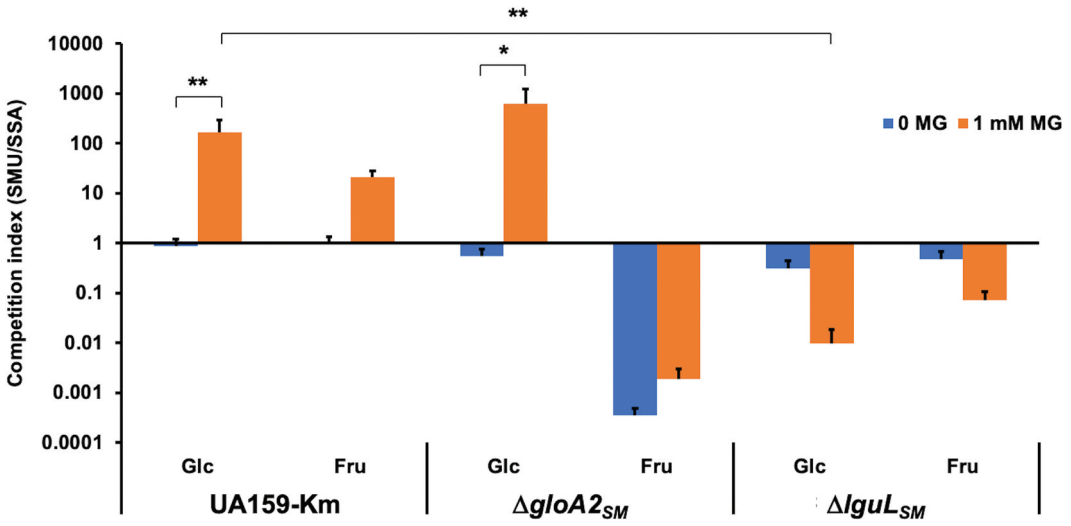

Figure 8. Competition between *S. mutans* and *S. sanguinis*. Exponential-phase cultures of UA159-Km (SM) and $\Delta gloA2_{SM}$ and $\Delta lguL_{SM}$ were each mixed with SS MMZ1945 at 1:1 ratio, followed by dilution at 1000-fold into FMC containing 20 mM or glucose or fructose, and incubation in 5% CO_2 atmosphere for 24 h. CFU enumeration at both the start and the end of the incubation resulted in competition indices of each species. Each strain was represented by at least three independent cultures, and the experiment was repeated twice with similar outcome. Statistical significance was assessed using three-way ANOVA (*$P < 0.05$; **$P < 0.01$) on a representative set of data.

observed in its competitiveness against SK36 (SS) in the absence of MG. When presented with 1 mM MG, strain Δ*lguL*$_{SM}$ showed about ~3000-fold reduction in competitiveness in a medium containing fructose, but its competition index was ~17,000-fold lower than the wild type on glucose.

Concluding remarks

We reported here a systematic characterization of streptococcal glyoxalase pathway that is essential for methylglyoxal and glyoxal tolerance in the oral microbiome, where RES compounds are constantly being produced by microbes and their host, especially during glycolysis. In response to our carbohydrate-rich Western diet and/or diabetic physiology, certain constituents of the oral microbiota could have evolved novel genetics that afford them advantages during competition with other organisms by becoming better at tolerating or detoxifying RES. Results of our study suggested that *S. mutans* could outcompete commensal streptococci in the presence of RES by several mechanisms. First, the genetic structure in SM where *lguL*$_{SM}$ finds itself includes an uncharacterized redox-modulating enzyme, a putative efflux pump protein, and a likely transcription regulator, all of which could aid in the expression and functionality of LguL in not-yet-understood ways. This genetic structure is present in a few other streptococcal species but absent in most commensals analyzed. The fact that the *lguL* mutants in SM and SS backgrounds showed comparable tolerance to MG strongly suggests that the SMU.1602–1625 locus and its regulation are critical to the apparently greater RES resistance of *S. mutans*. Second, although not yet fully understood, GloA2$_{SM}$ likely contributes to fructose and RES tolerance of SM in a manner directly related to cellular GSH::GSSG balance, and specific to the type of fructose metabolite as dictated by the PTS permeases that transport it (see Figure 9 for a working model). It is understood in mammalian cells that fructose oxidation in the presence of H_2O_2 worsens RES-mediated cellular injury [41,53]. It is thus probable that peroxigenic commensals such as SS and SG may be uniquely vulnerable to RES damage due to higher levels of cellular H_2O_2, especially when presented with fructose. Conversely, Gram-negative bacterium *E. coli* is known to activate a proton importer for cytoplasmic acidification as a means of blunting MG-induced cellular damage, in part by improving protonation of proteins or other cellular macromolecules [12]. Such a mechanism is likely absent in streptococci based on genomic analysis, raising the possibility that lactic acid bacteria as avid producers of organic acids might be innately more tolerant to RES effects. If so, cariogenic and aciduric pathobionts such as *S. mutans* and lactobacilli could naturally be even better protected from RES. Last, the glucose-PTS (EII^{Man}) of both *S. mutans* and *S. sanguinis* has been shown to regulate cellular bioenergetics and competitiveness, with significant distinctions in both underlying mechanism and phenotype [50,54]. The distinct effects on MG tolerance caused by *manL* deletion in these streptococci suggest different roles of PTS in RES-related gene regulation. We are actively pursuing these hypotheses to assess the contribution of RES to microbial dysbiosis, which may allow us to modulate microbiome ecology by targeting RES or RES-mediated gene regulation in biofilms. In conclusion, RES as an important group of metabolic byproducts are severely understudied in the context of oral microbiology, considering the etiology of dental caries and the epidemic of hyperglycemic disorders affecting the populations of the world. RES is likely more abundant when conditions favor caries development, thus the competitive advantage of *S. mutans* and other cariogenic pathobionts, if proven, in the presence of RES may be a major contributor to the ecological shifts that are characteristic of the development of cariogenic microbiomes. Future research into the contributions by, and mechanisms involved in regulating, RES-detoxifying pathways in pathobionts as well as oral microbiomes could provide important knowledge for oral health and better caries prevention, especially for diabetic individuals.

Materials and methods

Bacterial strains and culture conditions

S. mutans UA159, *S. sanguinis* SK36, *S. gordonii* DL1, their genetic derivatives (Table 3), and various other wild-type oral streptococcal isolates were first refreshed from frozen stocks by growing on BHI (Difco Laboratories, Detroit, MI) agar plates, then overnight in liquid BHI medium, before being diluted into fresh BHI, Tryptone-yeast extract medium (TY, 30 g of Tryptone and 5 g of yeast extract per liter), or FMC synthetic medium [55] that was supported with various carbohydrates as specified by each assay. Antibiotics were used, when necessary, at the following concentrations: kanamycin (Km) 0.5 to 1 mg/ml; erythromycin (Em) 5 to 10 μg/ml. All agar plates and liquid cultures were incubated at 37°C in an ambient atmosphere maintained with 5% CO_2 unless specified otherwise. Bacterial morphology in liquid cultures was assessed, without staining, using a Nikon Eclipse E400 microscope under the phase-contrast setting. For analysis of bacterial growth, BHI cultures of individual strains from the exponential phase were diluted 100-fold into FMC media in a 96-well plate, each at 200 μl volume and covered with 60 μl of mineral oil, before being loaded onto a Synergy 2 or Epoch 2 plate reader (BioTek, Agilent Technologies, Santa Clara, CA) maintained at 37°C, with optical density (λ = 600 nm, OD_{600}) data collected at 1-h interval. Autolysis assay was performed by following a previously published protocol detailed elsewhere [56]. Extracellular DNA in bacterial

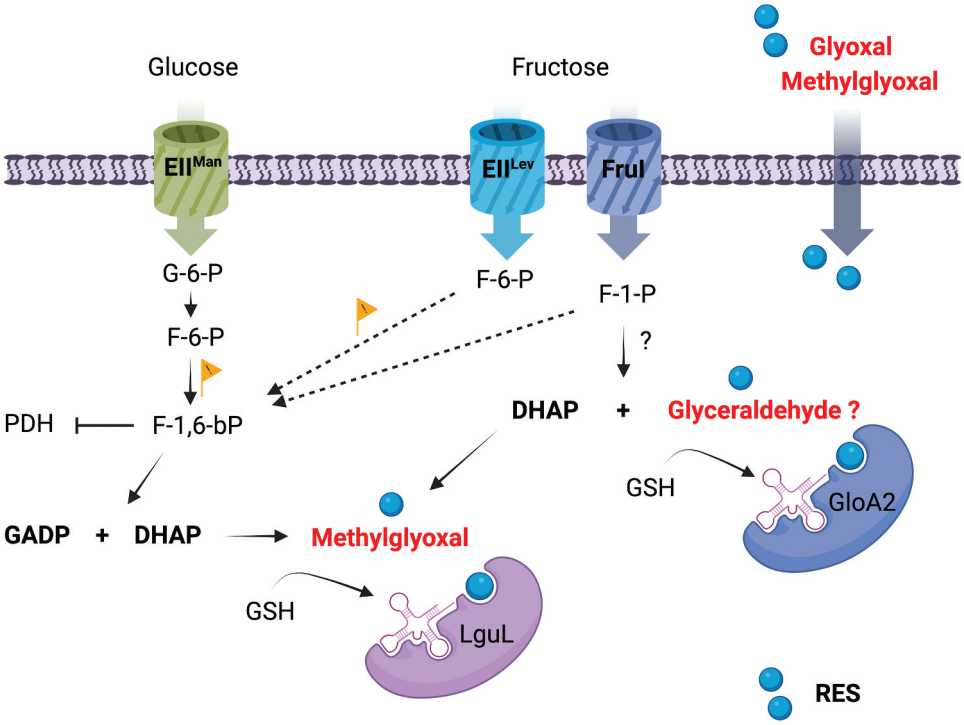

Figure 9. A diagram depicting RES metabolism in *S. mutans*. Also illustrated are PTS permeases that internalize glucose or fructose and the fate of their metabolites. Exogenous RES and RES produced during bacterial glycolysis are degraded by glyoxalase enzymes (LguL and potentially GloA2) in the presence of glutathione (GSH). We posit that fructose metabolism via F-1-P-specific PTS (FruI) contributes to excess RES production likely by 1) bypassing the allosteric check point at F-6-P phosphofructokinase, and 2) generation of glyceraldehyde through certain aldolase activity that targets F-1-P.

cultures was measured by combining 1:1 with a 5 µM solution of SYTOX Green nucleic acid stain (Thermo Fisher, Waltham, MA), followed by measurement of fluorescence (excitation/emission, 504/523 nm) using a Synergy H1 plate reader from BioTek (Winooski, VT) [35]. Antibiotics, sodium glutathione, methylglyoxal (MG) and glyoxal (GO) were purchased from MilliporeSigma (Burlington, MA).

Table 3. Strains used in this study (excluding oral commensal isolates in Table 1).

Strains	Relevant characteristics[a]	Source or reference
UA159	*S. mutans* wild type, *perR*$^+$	ATCC 700610
Δ*manL*$_{SM}$	UA159 *manL*::*Km*	From UA159
Δ*lguL*$_{SM}$	UA159 SMU.1603::*Km*	From UA159
Δ*lguL*$_{SM}$Com	Δ*lguL*$_{SM}$ complementation	From Δ*lguL*$_{SM}$
Δ*lguL*$_{SM}$/pIB-1112c	Δ*lguL*$_{SM}$ overexpressing *gloA2*$_{SM}$	From Δ*lguL*$_{SM}$
UA159/pIB-1112c	UA159 overexpressing *gloA2*$_{SM}$	From UA159
Δ*gloA2*$_{SM}$::*Km*	UA159 SMU.1112c::*Km*	From UA159
Δ*gloA2*$_{SM}$::*Em*	UA159 SMU.1112c::*Em*	From UA159
Δ*gloA2*$_{SM}$Com	Δ*gloA2*$_{SM}$ complementation	From Δ*gloA2*$_{SM}$::*Km*
Δ*gloA2*$_{SM}$/pIB-1112c	Δ*gloA2*$_{SM}$ overexpressing *gloA2*$_{SM}$	From Δ*gloA2*$_{SM}$::*Km*
Δ*gloB*$_{SM}$	UA159 SMU.1323::*Km*	From UA159
Δ*gloB*$_{SM}$Com	Δ*gloB*$_{SM}$ complementation	From Δ*gloB*$_{SM}$
Δ*gloA2*$_{SM}$/*fruI*	UA159 SMU.1112c::*Km fruI*::*Em*	From Δ*gloA2*$_{SM}$::*Km*
Δ*gloA2*$_{SM}$/*levD*	UA159 SMU.1112c::*Km levD*::*Em*	From Δ*gloA2*$_{SM}$::*Km*
Δ*gloA2*$_{SM}$/*lguL*$_{SM}$	UA159 SMU.1112c::*Km* SMU.1603::*Em*	From Δ*gloA2*$_{SM}$::*Km*
Δ*gloB*$_{SM}$/*lguL*$_{SM}$	UA159 SMU.1323::*Km* SMU.1603::*Em*	From Δ*gloB*$_{SM}$
Δ*gshAB*::*Km*	UA159 *gshAB*::*Km*	From UA159
Δ*gshAB*::*Em*	UA159 *gshAB*::*Em*	From UA159
Δ*gshAB*Com	Δ*gshAB* complementation	From Δ*gshAB*::*Km*
UA159-Km	*gtfA*::*Km*	[61]
SK36	*S. sanguinis* wild type	Kitten laboratory
Δ*manL*$_{SS}$	SK36 *manL*::*Km*	[54]
MMZ1945	SK36 *gtfP*::*Em*	From SK36
Δ*lguL*$_{SS}$	SK36 SSA_0962::*Km*	From SK36
Δ*gloA2*$_{SS}$	SK36 SSA_1625::*Km*	From SK36
Δ*gloB*$_{SS}$	SK36 SSA_0872::*Km*	From SK36
Δ*gloA2*$_{SS}$/*lguL*$_{SS}$	SSA_1625::*Km* SSA_0962::*Em*	From Δ*gloA2*$_{SS}$
DL1	*S. gordonii* wild type	ATCC 49818
Δ*manL*$_{SG}$	DL1 *manL*::*Km*	DL1 [57]

[a]*Em* and *Km*: resistance against erythromycin and kanamycin, respectively.

Construction of genetic mutants and complementation

Deletion of genes of interest was conducted by an allelic exchange strategy using a mutator DNA that was assembled (Gibson assembly) from two flanking sequences and an antibiotic marker in between, which would replace the target gene with the antibiotic cassette through homologous recombination [58]. Transformation of the wild type or mutant strains was achieved using naturally competent cells induced by treatment with competence-stimulating peptide (CSP) for respective species when growing in BHI. To improve scientific rigor, we routinely utilized a nonpolar kanamycin marker (*Km*) [59], which lacked a promoter sequence, and an erythromycin marker (*Em*) with its own promoter, to knock out the same gene separately. *Km* is known to have no polar effect but depends on local promoters for expression; *Em* has efficient expression, yet its promoter can in theory interfere with genes nearby. Both mutants were assayed for phenotypic change, although such results were not always included for the sake of brevity. Complementation analysis for phenotypic validation in mutants was carried out by a 'knock-in' strategy [54,60] that replaced in the mutator DNA the initial antibiotic cassette with an alternative marker, along with a wild-type copy of the target gene in between the two flanking fragments, followed by transformation of the said mutant. PCR amplification and assembly of the mutator DNA via Gibson assembly was performed according to a previously published protocol detailed elsewhere [54]. All genetic derivatives constructed in this study have been confirmed by PCR reactions targeting regions of interest, followed by Sanger sequencing. All oligonucleotides used in this procedure are listed in Table S1.

Minimum inhibitory concentration (MIC) assay

To measure the MIC for MG or GO, bacterial strains were first cultured overnight in BHI medium supplemented with 10 mM of potassium phosphate buffer (pH 7.2), then diluted 40-fold into 200 µl of FMC medium supported with 20 mM of glucose and varying concentrations of MG or GO. After incubating in an ambient incubator maintained with 5% of CO_2 at 37°C for 20–24 h, the optical density (OD_{600}) of the cultures was measured using a plate reader. Each strain was represented by at least three individual cultures. The minimum inhibitory concentration was defined as the levels above which OD_{600} remained unchanged relative to the blank. To report the increment in concentration used in the assay, the average MIC value is presented as a range, with the second value denoting the next immediate concentration above the actual MIC.

Planktonic growth competition assay

To evaluate bacterial competitiveness when cultivated together in a planktonic setting, a WT SM strain, UA159-Km [61] or other deletion mutants (Table 3), was marked with a Km marker, while an SS strain MMZ1945 was marked by an Em marker at the *gtfP* site [62]. Each strain was grown overnight in BHI (n = 3), followed by sub-culturing in the same BHI medium until the exponential phase (OD_{600} = 0.5). After mixing SM and SS strains at 1:1 volume, the cells were diluted 1000-fold into FMC medium supplemented with 20 mM of glucose or fructose, in addition to 0 or 1 mM of MG. The diluted cultures were then incubated for 24 h in 95% air and 5% CO_2 at 37°C. Both before (T_0) and after the 24-h incubation (T_{24}), the mixed cultures were subjected to a 15-s sonication at 100% power (FB120 water bath sonicator, Fisher Scientific), followed by serial dilution and plating onto selective agar plates containing either Km or Em. All plates were incubated for 2 days before CFU enumeration and calculation of competition indices. The competition index (SM over SS) was calculated as $[SM(T_{24})/SS(T_{24})]/[SM(T_0)/SS(T_0)]$, with values >1 indicating SM being more competitive than SS, and vice versa.

Biofilm assay

Development of biofilms was conducted on abiotic surfaces following previously published protocols [63]. In brief, bacterial cultures from mid-exponential phase (OD_{600} = 0.5) were diluted 100-fold into a biofilm medium BM [64] supplemented with 2 mM sucrose and 18 mM glucose (BMGS) or fructose (BMFS). The culture dilutions were then loaded, at 200 µl/well, onto a 96-well polystyrene microplate (Corning 3917) and incubated in 95% air and 5% CO_2 for 2 days without agitation. Biofilms were then stained with crystal violet to assess the total biomass, which was quantified by elution of the stain with 30% acetic acid and measurement of its optical density at 575 nm.

RNA extraction and RT-qPCR

RNA extraction and mRNA quantification was conducted by following a previously described protocol [65]. Briefly, bacterial cultures were prepared as above to exponential phase (OD_{600} = 0.4) in FMC medium containing 20 mM glucose, added 0 or 1 mM of MG and returned to incubation for 30 min, before being harvested by centrifugation. After treatment with RNAprotect Bacteria reagent,

bacterial cell envelope was disrupted by rapid homogenization in the presence of glass beads, SDS and acidic phenol and chloroform, followed by centrifugation to separate cell debris. Clarified cell lysate was processed using a Qiagen RNeasy kit and in-column treatment with a DNase I kit (Qiagen, Germantown, MD) for purification of total RNA. For RT-qPCR, a reverse transcription kit (iScript select cDNA synthesis kit, Bio-Rad, Hercules, CA) was used to create cDNA from the total RNA with gene-specific antisense primers (Table S1), followed by real-time PCR analysis using the CFX96 system and SYBR Green Supermix (Bio-Rad). Relative mRNA levels of each gene were quantified using the ΔCq method and an internal reference gene *gyrA*.

Statistical analysis and data availability

Statistical analysis of the data was carried out using the software of Prism (GraphPad of Dotmatics, San Diego, CA). Any data, strains and materials generated by this study will be available upon request from the authors for research or validation.

Disclosure statement

No potential conflict of interest was reported by the author(s).

Funding

This work was supported by the National Institute of Dental and Craniofacial Research [DE012236].

ORCID

Lin Zeng http://orcid.org/0000-0002-9269-2707
Robert A. Burne http://orcid.org/0000-0002-4234-0316

References

[1] Willenborg J, Goethe R. Metabolic traits of pathogenic streptococci. FEBS Lett. 2016;590(21):3905–3919.
[2] Lee C, Park C. Bacterial responses to glyoxal and methylglyoxal: reactive electrophilic species. Int J Mol Sci. 2017;18(1):169.
[3] Beisswenger PJ. Methylglyoxal in diabetes: link to treatment, glycaemic control and biomarkers of complications. Biochem Soc Trans. 2014;42(2):450–456.
[4] Chakraborty S, Karmakar K, Chakravortty D. Cells producing their own nemesis: understanding methylglyoxal metabolism. IUBMB Life. 2014;66(10):667–678.
[5] Allaman I, Bélanger M, Magistretti PJ. Methylglyoxal, the dark side of glycolysis. Front Neurosci. 2015;9:23.
[6] Leone A, Nigro C, Nicolò A, et al. The dual-role of methylglyoxal in tumor progression – novel therapeutic approaches. Front Oncol. 2021;11. doi: 10.3389/fonc.2021.645686
[7] Chaplen FWR, Fahl WE, Cameron DC. Evidence of high levels of methylglyoxal in cultured Chinese hamster ovary cells. Proc Natl Acad Sci USA. 1998;95(10):5533–5538.
[8] Maiden MF, Pham C, Kashket S. Glucose toxicity effect and accumulation of methylglyoxal by the periodontal anaerobe *Bacteroides forsythus*. Anaerobe. 2004;10(1):27–32.
[9] Rachman H, Kim N, Ulrichs T, et al. Critical role of methylglyoxal and AGE in mycobacteria-induced macrophage apoptosis and activation. PLoS One. 2006;1(1):e29.
[10] Booth IR, Ferguson GP, Miller S, et al. Bacterial production of methylglyoxal: a survival strategy or death by misadventure? Biochem Soc Trans. 2003;31(6):1406–1408.
[11] Cooper RA. Metabolism of methylglyoxal in microorganisms. Annu Rev Microbiol. 1984;38(1):49–68.
[12] Ozyamak E, Black SS, Walker CA, et al. The critical role of S-lactoylglutathione formation during methylglyoxal detoxification in *Escherichia coli*. Mol Microbiol. 2010;78(6):1577–1590.
[13] Zhang MM, Ong CL, Walker MJ, et al. Defence against methylglyoxal in group a *Streptococcus*: a role for glyoxylase I in bacterial virulence and survival in neutrophils? Pathog Dis. 2016;74(2):ftv122.
[14] Korithoski B, Levesque CM, Cvitkovitch DG. Involvement of the detoxifying enzyme lactoylglutathione lyase in *Streptococcus mutans* aciduricity. J Bacteriol. 2007;189(21):7586–7592.
[15] Reiger M, Lassak J, Jung K. Deciphering the role of the type II glyoxalase isoenzyme YcbL (GlxII-2) in *Escherichia coli*. FEMS Microbiol Lett. 2015;362(2):1–7.
[16] MacLean MJ, Ness LS, Ferguson GP, et al. The role of glyoxalase I in the detoxification of methylglyoxal and in the activation of the KefB K + efflux system in *Escherichia coli*. Mol Microbiol. 1998;27(3):563–571.
[17] Anaya-Sanchez A, Feng Y, Berude JC, et al. Detoxification of methylglyoxal by the glyoxalase system is required for glutathione availability and virulence activation in *Listeria monocytogenes*. PLoS Pathog. 2021;17(8):e1009819.
[18] Sun H, Saeedi P, Karuranga S, et al. IDF Diabetes Atlas: global, regional and country-level diabetes prevalence estimates for 2021 and projections for 2045. Diabetes Res Clin Pract. 2022;183:109119.
[19] Preshaw PM, Alba AL, Herrera D, et al. Periodontitis and diabetes: a two-way relationship. Diabetologia. 2012;55(1):21–31.
[20] Ferizi L, Bimbashi V, Kelmendi J. Association between metabolic control and oral health in children with type 1 diabetes mellitus. BMC Oral Health. 2022;22(1):502.
[21] Syrjälä AM, Niskanen MC, Ylöstalo P, et al. Metabolic control as a modifier of the association between salivary factors and dental caries among diabetic patients. Caries Res. 2003;37(2):142–147.
[22] De lima AKA, Amorim Dos Santos J, Stefani CM, et al. Diabetes mellitus and poor glycemic control increase the occurrence of coronal and root caries: a systematic review and meta-analysis. Clin Oral Investig. 2020;24(11):3801–3812.
[23] Song IS, Han K, Park YM, et al. Type 2 diabetes as a risk indicator for dental caries in Korean adults: the 2011–2012 Korea national health and nutrition examination survey. Community Dent Health. 2017;34(3):169–175.
[24] Schmolinsky J, Kocher T, Rathmann W, et al. Diabetes status affects long-term changes in coronal caries - the SHIP study. Sci Rep. 2019;9(1):15685.

[25] Beheshti M, Badner V, Shah P, et al. Association of diabetes and dental caries among U.S. adolescents in the NHANES dataset. Pediatr Dent. 2021;43(2):123–128.
[26] Quivey RG, Kuhnert WL, Hahn K. Genetics of acid adaptation in oral streptococci. Crit Rev Oral Biol Med. 2001;12(4):301–314.
[27] Bowen WH, Burne RA, Wu H, et al. Oral biofilms: pathogens, matrix, and polymicrobial interactions in microenvironments. Trends Microbiol. 2018;26 (3):229–242.
[28] Burne RA. Oral Streptococci … products of their environment. J Dent Res. 1998;77(3):445–452.
[29] Rice KC, Turner ME, Carney OV, et al. Modification of the Streptococcus mutans transcriptome by LrgAB and environmental stressors. Microb Genom. 2017;3 (2):e000104.
[30] Tinder EL, Faustoferri RC, Buckley AA, et al. Analysis of the *Streptococcus mutans* proteome during acid and oxidative stress reveals modules of protein coexpression and an expanded role for the TreR transcriptional regulator. mSystems. 2022;7(2):e01272–21.
[31] Kim TH, Park SC, Lee K-C, et al. Structural and DNA-binding studies of the PadR-like transcriptional regulator BC1756 from *Bacillus cereus*. Biochem Biophys Res Commun. 2019;515(4):607–613.
[32] Velsko IM, Chakraborty B, Nascimento MM, et al. Species designations belie phenotypic and genotypic heterogeneity in oral streptococci. mSystems. 2018;3 (6):e00158–18.
[33] Culp DJ, Hull W, Bremgartner MJ, et al. *In vivo* colonization with candidate oral probiotics attenuates colonization and virulence of *Streptococcus mutans*. Appl Environ Microbiol. 2020;87(4). doi: 10.1128/AEM.02490-20
[34] Biswas I, Jha JK, Fromm N. Shuttle expression plasmids for genetic studies in *Streptococcus mutans*. Microbiology. 2008;154(8):2275–2282.
[35] Zeng L, Burne RA. Essential roles of the sppRA fructose-phosphate phosphohydrolase operon in carbohydrate metabolism and virulence expression by Streptococcus mutans. J Bacteriol. 2019;201(2):e00586–18.
[36] Zeng L, Chakraborty B, Farivar T, et al. Coordinated regulation of the EII man and fruRKI operons of Streptococcus mutans by global and fructose-specific pathways. Appl Environ Microbiol. 2017;83(21): e01403–17.
[37] Zeng L, Burne RA. Multiple sugar: phosphotransferase system permeases participate in catabolite modification of gene expression in *Streptococcus mutans*. Mol Microbiol. 2008;70(1):197–208.
[38] Zeng L, Burne RA. Comprehensive mutational analysis of sucrose-metabolizing pathways in *Streptococcus mutans* reveals novel roles for the sucrose phosphotransferase system permease. J Bacteriol. 2013;195 (4):833–843.
[39] Puccio T, Misra BB, Kitten T. Time-course analysis of *Streptococcus sanguinis* after manganese depletion reveals changes in glycolytic and nucleic acid metabolites. Metabolomics. 2021;17(5):44.
[40] Aragno M, Mastrocola R. Dietary sugars and endogenous formation of advanced glycation endproducts: emerging mechanisms of disease. Nutrients. 2017;9 (4):385.
[41] Manini P, La Pietra P, Panzella L, et al. Glyoxal formation by Fenton-induced degradation of carbohydrates and related compounds. Carbohydr Res. 2006;341(11):1828–1833.
[42] Lee O, Bruce WR, Dong Q, et al. Fructose and carbonyl metabolites as endogenous toxins. Chem Biol Interact. 2009;178(1–3):332–339.
[43] Zheng X, Zhang K, Zhou X, et al. Involvement of *gshAB* in the interspecies competition within oral biofilm. J Dent Res. 2013;92(9):819–824.
[44] Usui T, Shizuuchi S, Watanabe H, et al. Cytotoxicity and oxidative stress induced by the glyceraldehyde-related Maillard reaction products for HL-60 cells. Biosci Biotech Biochem. 2004;68(2):333–340.
[45] Sato Y, Yamamoto Y, Kizaki H, et al. Isolation and sequence analysis of the pmi gene encoding phosphomannose isomerase of *Streptococcus mutans*. FEMS Microbiol Lett. 1993;114(1):61–66.
[46] Abranches J, Chen YY, Burne RA. Characterization of Streptococcus mutans strains deficient in EIIAB Man of the sugar phosphotransferase system. Appl Environ Microbiol. 2003;69(8):4760–4769.
[47] Nakayama K. Nucleotide sequence of *Streptococcus mutans* superoxide dismutase gene and isolation of insertion mutants. J Bacteriol. 1992;174(15):4928–4934.
[48] Seaton K, Ahn S-J, Burne RA. Regulation of competence and gene expression in *Streptococcus mutans* by the RcrR transcriptional regulator. Mol Oral Microbiol. 2014;30 (2):147–159.
[49] Zeng L, Burne RA. Sucrose- and fructose-specific effects on the transcriptome of *Streptococcus mutans*, as determined by RNA sequencing. Appl Environ Microbiol. 2016;82(1):146–156.
[50] Abranches J, Candella MM, Wen ZT, et al. Different Roles of EIIAB man and EII Glc in regulation of energy metabolism, biofilm development, and competence in Streptococcus mutans. J Bacteriol. 2006;188 (11):3748–3756.
[51] Busuioc M, Buttaro BA, Piggot PJ. The pdh operon is expressed in a subpopulation of stationary-phase bacteria and is important for survival of sugar-starved Streptococcus mutans. J Bacteriol. 2010;192 (17):4395–4402.
[52] Korithoski B, Lévesque CM, Cvitkovitch DG. The involvement of the pyruvate dehydrogenase E1Î± subunit, in *Streptococcus mutans* acid tolerance. FEMS Microbiol Lett. 2008;289(1):13–19.
[53] Feng CY, Wong S, Dong Q, et al. Hepatocyte inflammation model for cytotoxicity research: fructose or glycolaldehyde as a source of endogenous toxins. Arch Physiol Biochem. 2009;115(2):105–111.
[54] Zeng L, Walker AR, Lee K, et al. Spontaneous mutants of *Streptococcus sanguinis* with defects in the glucose-phosphotransferase system show enhanced post-exponential-phase fitness. J Bacteriol. 2021;203(22):JB0037521.
[55] Terleckyj B, Willett NP, Shockman GD. Growth of several cariogenic strains of oral streptococci in a chemically defined medium. Infect Immun. 1975;11 (4):649–655.
[56] Ahn SJ, Burne RA. Effects of oxygen on biofilm formation and the AtlA autolysin of *Streptococcus mutans*. J Bacteriol. 2007;189(17):6293–6302.
[57] Tong H, Zeng L, Burne RA. The EIIAB man phosphotransferase system permease regulates carbohydrate catabolite repression in Streptococcus gordonii. Appl Environ Microbiol. 2011;77(6):1957–1965.
[58] Lau PC, Sung CK, Lee JH, et al. PCR ligation mutagenesis in transformable streptococci: application and efficiency. J Microbiol Methods. 2002;49(2):193–205.
[59] Seaton K, Ahn SJ, Sagstetter AM, et al. A transcriptional regulator and ABC transporters link stress tolerance, (p)

PPGPP, and genetic competence in *Streptococcus mutans*. J Bacteriol. 2011;193(4):862–874.
[60] Zheng L, Chen Z, Itzek A, et al. Catabolite control protein a controls hydrogen peroxide production and cell death in *Streptococcus sanguinis*. J Bacteriol. 2011;193(2):516–526.
[61] Chen L, Chakraborty B, Zou J, et al. Amino sugars modify antagonistic interactions between commensal oral streptococci and *Streptococcus mutans*. Appl Environ Microbiol. 2019;85(10):e00370–19.
[62] Zeng L, Walker AR, Burne RA, et al. Glucose phosphotransferase system modulates pyruvate metabolism, bacterial fitness, and microbial ecology in oral streptococci. J Bacteriol. 2022;205(1):e0035222.
[63] Wen ZT, Burne RA. Functional genomics approach to identifying genes required for biofilm development by *Streptococcus mutans*. Appl Environ Microbiol. 2002;68(3):1196–1203.
[64] Loo CY, Corliss DA, Ganeshkumar N. *Streptococcus gordonii* biofilm formation: identification of genes that code for biofilm phenotypes. J Bacteriol. 2000;182(5):1374–1382.
[65] Moye ZD, Zeng L, Burne RA. Modification of gene expression and virulence traits in *Streptococcus mutans* in response to carbohydrate availability. Appl Environ Microbiol. 2014;80(3):972–985.